

Development of a Mathematical Theoretical Model and Simulation of the Electromechanical System for Wave Energy Harvesting

P. Valdez, M. Pelissero, A. Haim, F. Muiño, F. Galia, R. Tula

Abstract—As a result of the studies performed on the wave energy resource worldwide, a research project was set up to harvest wave energy for its conversion into electrical energy. Within this framework, a theoretical model of the electromechanical energy harvesting system, developed with MATLAB's Simulink software, will be provided. This tool recreates the site conditions where the device will be installed and offers valuable information about the amount of energy that can be harnessed. This research provides a deeper understanding of the utilization of wave energy in order to improve the efficiency of a 1:1 scale prototype of the device.

Keywords—Electromechanical device, modeling, renewable energy, sea wave energy, simulation.

I. INTRODUCTION

THE research project entitled “Wave Energy Harnessing” entails three work stages: the first consisted of the elaboration of the conceptual, theoretical proposal for the harvesting of the referred resource by means of an innovative design which resulted in a patent and a 1:20 scale functional model. In the second stage, a 1:10 scale prototype is currently under development and, as a result, the 1:1 model is being developed as well. A simulation model that best represents the dynamic behavior of the system is currently under development as part of the second stage. These data will be used during the third stage to validate the model developed. Finally, the third stage will consist of the design and construction of the full-scale model.

The theoretical framework is described below. Such description is based on an electro-mechanical system for sea wave energy harvesting by means of a buoy that is fixed to the energy conversion device. The wave energy captured by the buoy is transmitted to the kinematic chain and to the electricity generator. To understand the energy transmission mechanics better, the system was analyzed by dividing it into different parts, as follows:

II. BUOY-ARM SYSTEM

The arm, weighing $P_{BR} = m_{BR}g$ [N] and with a length of L [m], spins around the center O . The buoy, weighing $P_b = m_b g$ [N] and with a height of h_b [m], hangs from the end of the arm at the height of z_b [m] from the reference point. Fig. 1.

Dr. Pablo Valdez is with the National Technological University, Argentina (e-mail: pablopatriovaldez@yahoo.com).

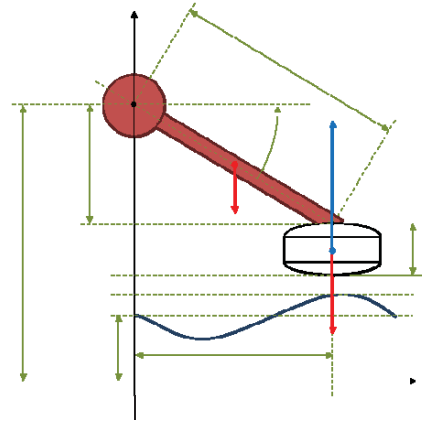


Fig. 1 Buoy-arm system

Applying Newton's second law $\sum_{i=1}^N F_i d_i + \sum_{i=1}^K T_i = J \frac{d^2\theta}{dt^2}$, the resulting expression is (1):

$$E x_B - P_B x_B - P_{BR} \frac{x_B}{2} - T'_E - T_R = J \frac{d^2\theta}{dt^2} \quad (1)$$

Buoy force is E [N], T'_E [Nm] is the resistant torque of the electrical generator related to the speed of the arm-buoy set, T_R [Nm] is the resistant torque resulting from friction, and T_R [Nm] is the system's equivalent moment of inertia. Considering that $x_B = L \cos(\theta)$, from expression (1) the resulting expression is (2):

$$(E - P_B - P_{BR}/2) L \cos(\theta) - T'_E - T_R = J \frac{d^2\theta}{dt^2} \quad (2)$$

The block diagram corresponding to the buoy-arm set model proposed is shown in Fig. 2. This diagram may be used with any numerical simulation software to analyze the behavior of the equipment under different sea wave conditions. For example, if we want to know what happens at a given site, we enter wave height (z_A), and we will immediately obtain the angle (ang_b in rad.) and the position of the arm (z_b and x_b).

III. BUOY FORCE

Buoy force depends on its volume and submerging depth,

which results in a non-linear expression (3) depending on the difference between the water and buoy heights $z_A - z_B$:

$$E = f(z_A - z_B) = \begin{cases} 0 & \text{si } z_A - z_B \leq 0 \\ 0 \leq E \leq E_{\max} & \text{si } 0 \leq z_A - z_B \leq h_B \\ E_{\max} & \text{si } z_A - z_B \geq h_B \end{cases} \quad (3)$$

For example, the force function for the buoy shape of the figure might be seen in Fig. 3. The position of the buoy base z_B is represented by expression (4):

$$z_B = z_{B0} + L \sin(\theta) - h_B \quad (4)$$

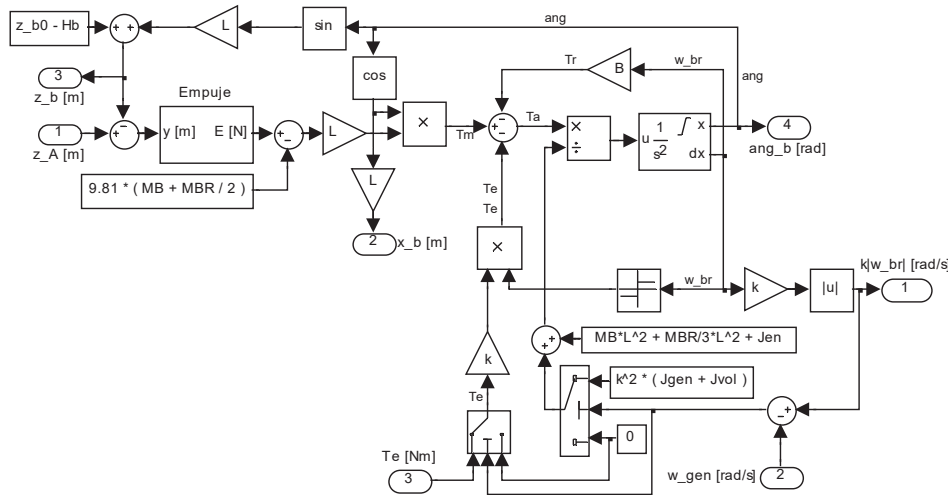


Fig. 2 Block diagram of the Buoy-arm model

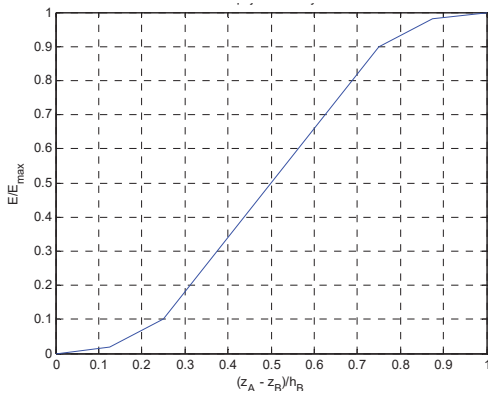


Fig. 3 Buoy force function

IV. PLANETARY MULTIPLIER

The planetary multiplier is represented simply by the quotient of the speeds k on the output (generator) and on the input (arm and buoy) through expression (5):

$$k = \frac{\omega_G}{\omega} \quad (5)$$

Losses caused by friction are included in the coefficient B , described in (2) where T_R [Nm] is the resistant torque resulting from friction.

V. FRICTION AND ELECTRIC TORQUE

Mechanical friction of the arm-buoy set may be considered proportional to the angular velocity $\omega = \frac{d\theta}{dt}$ through expression (6):

$$T_R = B \omega = B \frac{d\theta}{dt} \quad (6)$$

This friction always opposes the motion and therefore, its sign changes depending on the angular velocity. The electric resistant torque is applied to the arm-buoy system when it is interacting with the generator. Under these conditions, the torque is proportional to the electrical power generated and inversely proportional to the generator's spin velocity, expression (7):

$$T'_E = kT_E = \begin{cases} k \frac{P_E}{\omega_G} \text{sgn}(\omega) & \text{if arm pulls} \\ 0 & \text{if it spins freely} \end{cases} \quad (7)$$

Due to the fact that the generator always turns in the same direction by means of the reverse gear, the resistant torque must be multiplied by the signum function of ω to result in opposition every time.

VI. EQUIVALENT MOMENT OF INERTIA

Equivalent moment of inertia will depend on whether the arm is interacting with the generator or not. Its expression (8) is:

$$J \cong \begin{cases} m_b L^2 + \frac{1}{3} m_{BR} L^2 + J_{EN} + k^2 (J_G + J_V) & \text{if arm pulls} \\ m_b L^2 + \frac{1}{3} m_{BR} L^2 + J_{EN} & \text{if it spins freely} \end{cases} \quad (8)$$

where J_{EN} is the moment of inertia of the planetary gears, J_G is the moment of inertia of the generator, and J_V is the moment of inertia of the flywheel.

VII. REVERSE GEAR AND COUPLING

From the generator's perspective, the reverse gear of the arms is equivalent to the calculation of the angular speed module and its multiplication by the planetary amplification.

VIII. ELECTRICAL GENERATOR AND FLYWHEEL

The electrical generator-inertial flywheel set will turn to a minimum speed equal to the maximum speed between arms. In this case, the arm is interacting with the system. If the speeds of the arms are lower than the generator flywheel speed, this system will evolve according to its movement equation in expression (9):

$$\omega_G = \begin{cases} \max(\omega_1, \omega_2) & \text{if arm pulls} \\ -T_E - B_G \omega_G = (J_G + J_V) \frac{d\omega_G}{dt} & \text{if it spins freely} \end{cases} \quad (9)$$

where T_E [Nm] is the resistant torque of the electrical generator and B_G [N s] is the resistant torque resulting from the friction.

Numerical modeling has been used in some wave energy converters (WECs), which allowed comparing the theoretical results with those obtained from experimental testing [1] in order to better study them. Commercial projects using WEC technology include devices such as different buoy concepts [2], Oscillating-Water-Column (OWC) plants like LIMPET in Scotland [3] or Mutriku in Spain [4], the Pelamis in Portugal [5], overtopping WEC types like the Wave Dragon [6], and the Wave Star device in Denmark [7].

In our case, the simulation control is performed through a specifically scheduled application [8], similar to the SCADA system of the wave energy plant operator. Fig. 4.

Through this application, the simulation parameters, the sea wave conditions at the site of study, the dimensional characteristics of the equipment and its method of control can be modified Fig. 5.

IX. EXPERIMENTAL STAGE

The results of the real-time simulation can be visualized through time series of all physical variables (including arms position, wave height, the rotational speed of the generator or electrical power) or through an animated tridimensional model which response to the cited variables Figs. 6 and 7.

This device [9] consists of two shipbuilding steel buoys (1). They are hollow and filled with polyurethane foam, and they weigh 10 tons each. Such buoys generate a thrust equal to their weight, Archimedes principle, thus keeping the torque constant in the axis of the lever arm (2), both in the ascent and descent buoy.

As a consequence of the simulated waves and the buoys movement, the mechanical variables of the following graphs are generated Fig. 8. The reaction of the generator results in variable electrical power but with a mean value defined in relation to the waves.

Fig. 10 shows the control display: commands, equipment behavior in two views and results obtained from the variation of power in time.

X. RESULTS

The results of the simulation are expressed in Fig. 11. The graph shows the paths of the output shaft revolutions of each arm's reverse gear in red and blue, and the path of the generator shaft coupled to the inertia flywheels is expressed in green.

Graph in Fig. 12 shows the variation of power in accordance to time in red.

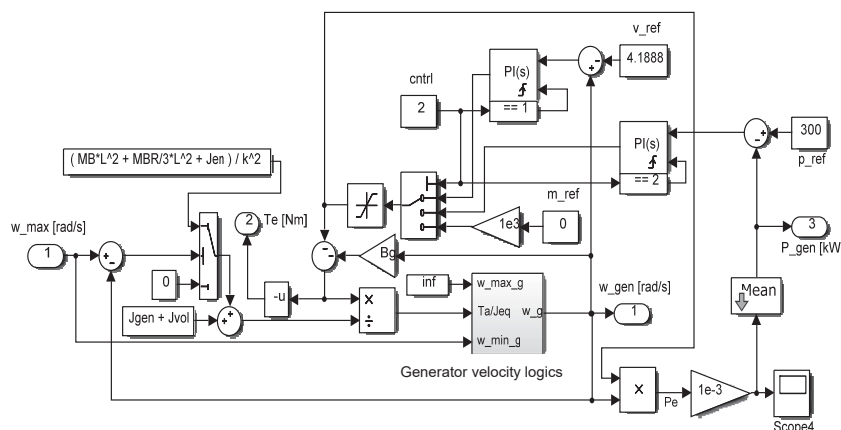


Fig. 4 Simulation control of the wave energy plant operator

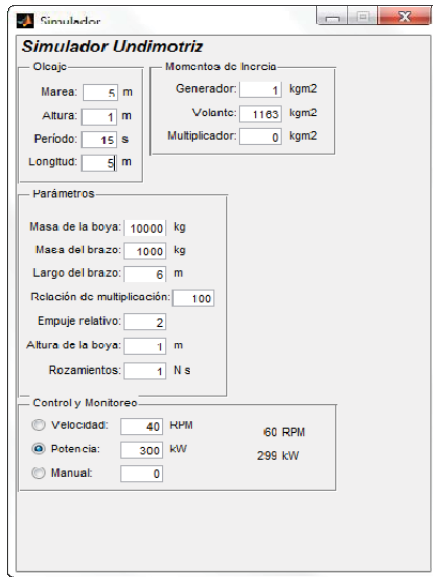


Fig. 5 Configuration and control display



Fig. 6 Physical Simulation of the tridimensional model

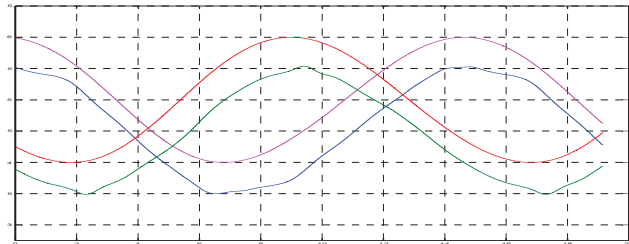


Fig. 7 Wave height and buoy height (accompanying waves)

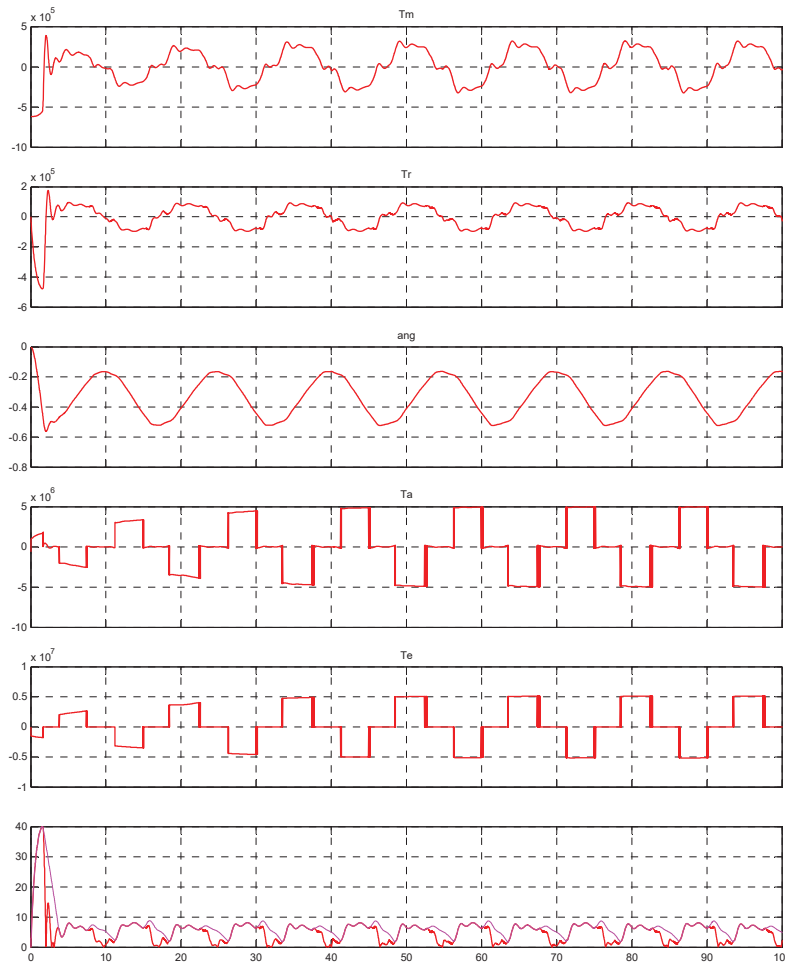


Fig. 8 Arm torque, resistant torque, arm angle, accelerating coupling, electromagnetic coupling, speed of the generator

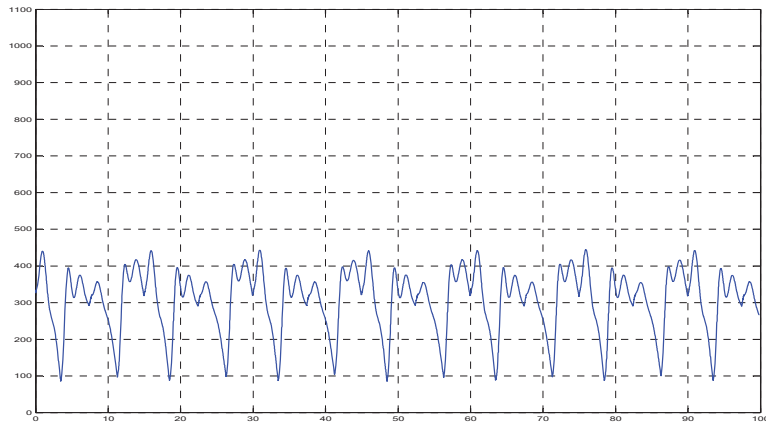


Fig. 9 Electrical power in kW

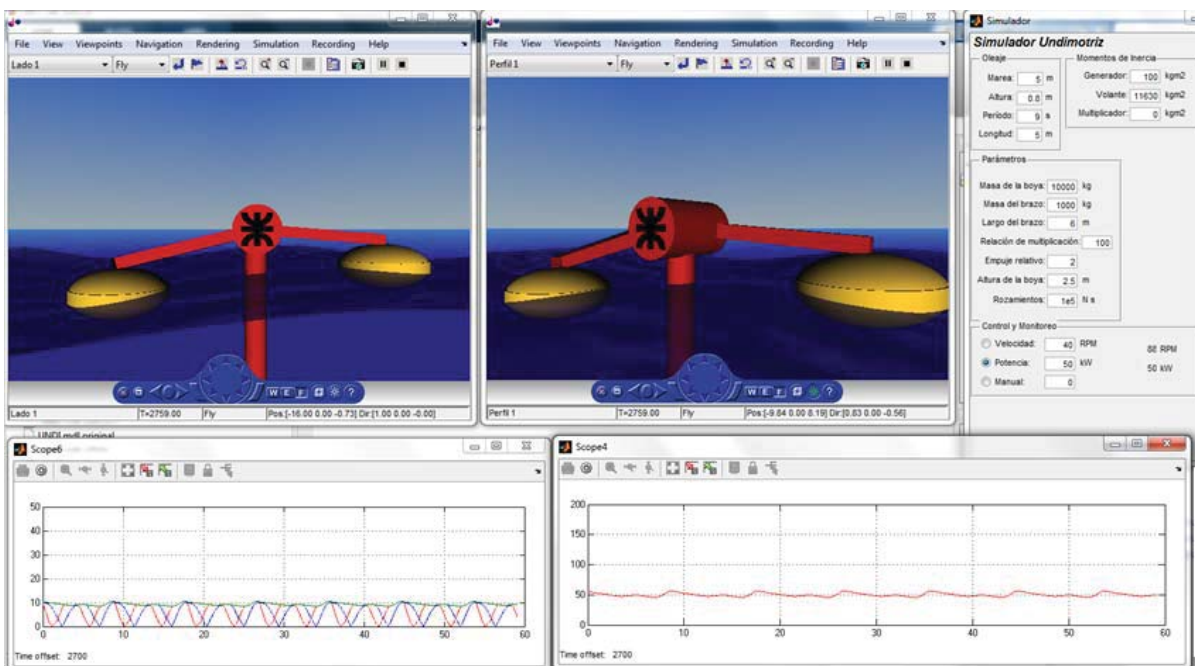


Fig. 10 An example of Simulation control panel (Details are shown in Fig. 8)

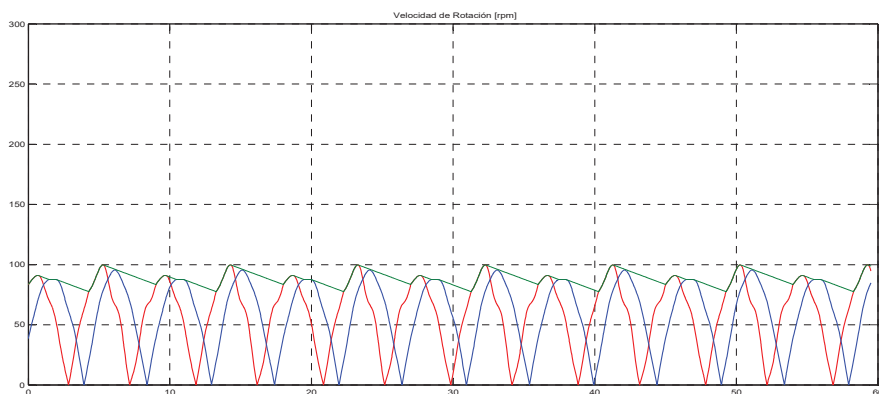


Fig. 11 Graphs showing the paths of the reverse gear output shaft and the inertia flywheel and generator shaft

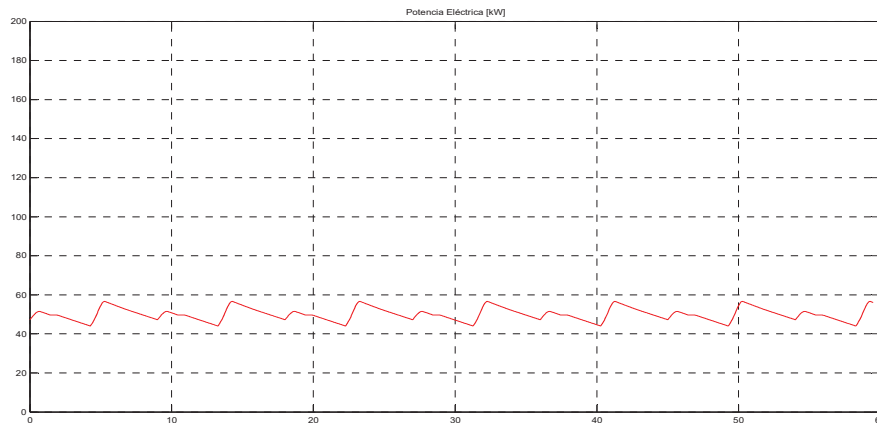


Fig. 12 Graph showing the variation of generator power in relation to time

XI. DISCUSSION

Although this simulation allows saving resources, it is essential to validate the simulation with experiments and tests of the said equipment through field tests. In order to put the proposed theory into practice, a reduced scale power-train (1:20) was constructed [10] so that the operation of the system could be verified. For such purpose, we are finishing with the construction of the equipment at 1:10 scale to be tested in the wave tank of the Instituto Nacional del Agua.

XII. CONCLUSION

The use of the proposed simulation system allows, on the one hand, to study the behavior under diverse climatic conditions of the selected site as well as to take it to other sites; and on the other, to obtain the results of relevant parameters for the best theoretical design. The simulation reacted exactly like the theoretically developed model and converted a variable oscillating movement and a quasi-constant movement within a certain range of design, which allows the generator to work within its design range and to generate electrical energy efficiently.

ACKNOWLEDGEMENT

The authors thank Guillermo Oliveto, Ana Julia Lifschitz, Diego Gagnieri, Emiliano Cirelli, Mariano Montoneri, Gustavo De Vita, Ezequiel Heinke, Emiliano Cirelli, Tomás Santino, Macarena Balbiani and Sebastián Bernal.

REFERENCES

- [1] Zurkinden, A. S., Kramer, M., Teimouri, M., & Alves, M. (2012). Comparison between numerical modeling and experimental testing of a point absorber WEC using linear power take-off system. Proceedings of the ASME 2012 31st International Conference on Ocean, Offshore and Arctic Engineering OMAE 2012 June 10-15, 2012, Rio de Janeiro, Brazil OMAE2012-83692.
- [2] Falnes, J. Ocean waves and oscillating systems: linear interactions including wave energy extraction. Cambridge: Cambridge University Press. 2002.
- [3] Setoguchi, T., & Takao, M. (2006). Current status of self-rectifying air turbines for wave energy conversion. Energy Conversion and Management, 2382-2396.

- [4] Tease, W., Lees, J., & Hall, A. (2007). Advances in Oscillating Water Column Air Turbine development. Proceedings of the 7th European Wave and Tidal Energy Conference. Oporto (Portugal).
- [5] Pelamis Wave Power. <http://www.emec.org.uk/about-us/wave-clients/pelamis-wave-power/>
- [6] WaveDragon. http://www.wavedragon.net/index.php?option=com_content&task=view&id=28&Itemid=46
- [7] Wavestar Energy. <http://wavestarenergy.com/projects>
- [8] Matlab Simulink. (2013) of The MathWorks, Inc.
- [9] Pelissero M.; Haim A.; Tula R.; Galia F. & Muiño F. (2014) Descripción del dispositivo de aprovechamiento de la energía undimotriz. Buenos Aires, Argentina. ISSN: 1667-8400.
- [10] Haim, A.; Tula, R. (2011). Mecanismo de accionamiento para una máquina electromecánica transformadora de energía undimotriz en energía eléctrica. Buenos Aires, Argentina. ISSN: 0325-6545.